Indian Journal of Advanced Chemistry (IJAC)
ISSN: 2582-8975 (Online), Volume-6 Issue-2, October 2026

Synthesis, Physicochemical Characterization, and Metal Complexation of Novel Azo-Diketone Sulfonamide Derivatives

Noor A. Abdulrazzaq*

Abstract: ***This study synthesised two novel azo-diketone ligands (N1 and N2) based on sulfonamides, investigated their complexation with copper(II) and nickel(II) ions, and elucidated the structural properties and coordination patterns of the resulting compounds. We prepared the ligands via a standard diazotisation and coupling protocol, and synthesised the solid metal complexes by direct coordination at a 2:1 molar ratio. We characterised the complex systems using a multi-analytical approach and assessed their biological activity. The results showed the formation of (2:1) complexes with high thermal stability. The copper complexes exhibited a planar square structure, while the nickel complexes had an octahedral structure. Bioassays showed that mineralisation significantly enhanced antioxidant and antimicrobial activity. The N2Cu complex had an IC50 of 16.8 µg/mL, close to ascorbic acid. Copper complexes also exhibited low minimum inhibitory concentration (MIC) values, as low as 0.5 mg/mL, against S. aureus. The N2Cu complex surpassed this, with an inhibition zone diameter of 28 mm, demonstrating high efficacy against bacteria and fungi. The results confirm the potential use of copper-sulfonamide complexes as therapeutic agents and highlight the crucial role of metal ion selection in metal drug design.***

Keywords: ***Azo-Diketone, Sulfonamide, Copper Complex, Antioxidant, Antimicrobial.***

Nomenclature:

Common Abbreviations, Technical Abbreviations:

CHN: Carbon, Hydrogen, Nitrogen (Elemental Analysis)
FTIR / FT-IR: Fourier-Transform Infrared Spectroscopy
IR: Infrared
UV–Vis: Ultraviolet–Visible Spectroscopy
NMR: Nuclear Magnetic Resonance
^{1}H NMR: Proton Nuclear Magnetic Resonance
TGA: Thermogravimetric Analysis
TLC: Thin-Layer Chromatography
GC/MSD: Gas Chromatography/Mass Selective Detector
EI: Electron Ionization
DPPH: 2,2-Diphenyl-1-Picrylhydrazyl
MIC: Minimum Inhibitory Concentration
IC_{50}: Half-Maximal Inhibitory Concentration
CLSI: Clinical and Laboratory Standards Institute
ROS: Reactive Oxygen Species
DNA: Deoxyribonucleic Acid
KBr*: Potassium Bromide*
DMSO: Dimethyl Sulfoxide
TMS: Tetramethylsilane
HOD: Hydrogen Deuterium Oxide (HDO/HOD Signal)
Comp: Compound
M.P.: Melting point
Calc.: Calculated

Greek Letters and Spectral Symbols:

µ_eff: Effective Magnetic Moment
Λ_m: Molar Conductivity
ν / ν: Vibrational Frequency/Band
π→π*, n→π*: Electronic Transitions

Chemical Formulas, Compound Nomenclature, and Scientific Symbols:

N1, N2: Study Ligand Labels
N1Cu, N1Ni, N2Cu, N2Ni: Labels for the Ligand–Metal Complexes
L: M / L/M: Ligand-to-Metal Ratio
$[M+H]^+$: Protonated Molecular Ion
Ar–H: Aromatic Proton
s/m: Singlet/Multiple
m/z: Mass-to-Charge Ratio

Units of Measurement

B.M.: Bohr Magneton
Ppm: Parts Per Million
M: Molar; Moles Per Litre
mM: Millimolar
eV: Electron Volt
°C: Degree Celsius
Nm: Nanometre
Mm: Millimetre
µg/mL: Microgram per Millilitre
Ω^{-1} cm² mol^{-1}: Reciprocal Ohm × Square Centimetre × Reciprocal Mole

Scientific Names of Microorganisms

S. aureus: Staphylococcus aureus
E. coli: Escherichia coli
C. albicans: Candida Albicans
A. Niger: Aspergillus Niger

Manuscript received on 05 September 2026 | First Revised Manuscript received on 12 September 2026 | Second Revised Manuscript received on 02 October 2026 | Manuscript Accepted on 15 October 2026 | Manuscript published on 30 October 2026.

*Correspondence Author(s)
Dr. **Noor A. Abdulrazzaq***, Ministry of Education, Directorate General of Education of Basrah, 61001, Basrah, Iraq. Email ID: noor.abd@gmail.com, mustafafadil837@gmail.com, ORCID ID: 0009-0004-9706-6352.

© The Authors. Published by Lattice Science Publication (LSP). This is an open-access article under the CC-BY-NC-ND license. https://creativecommons.org/licenses/by-nc-nd/4.0/

I. INTRODUCTION

Over the last 100 years, azo compounds have attracted significant attention in chemical research for their broad applications as synthetic dyes, pigments, and high-tech nonlinear-optics materials [1]. Beyond their industrial utility, azo derivatives that incorporate heterocyclic or sulfonamide structures have also attracted substantial interest in medicinal chemistry [2]. Sulfa drugs, also known as sulfonamides, are known for their broad-spectrum antimicrobial, anti-inflammatory, and diuretic effects [3]. The synergistic effect of the azo linkage (-N=N) with sulfonamide functionality frequently enhances the biological efficacy of the resulting compounds [4]. Azo ligands have found extensive application in coordination chemistry, expanding their functional scope. Azo dyes are transition-metal complexes with remarkable thermal stability, light fastness, and unique catalytic properties [5]. Introducing

© Copyright: All rights reserved.

β-diketone structures into the azo framework is especially important because it adds new donor groups, including carbonyl oxygens, that can coordinate with transition metals such as copper and nickel to form stable chelate rings [6]. Nickel(II) and copper(II) complexes are particularly attractive because of their diverse stereochemistry and biochemical applications as metalloenzyme mimics [7]. Recent literature highlights the synthesis of numerous sulfonamide-functionalized azo–metal structures and their promising potential as effective antibacterial and antifungal agents [8]. For instance, sulfonamide derivatives' affinity for transition metals can significantly increase their lipophilicity, which can, in turn, improve their penetration across microbial cell membranes [9].

In addition, the spectral characteristics of such complexes, including their electronic transitions and vibrations, provide important information about the electronic nature of the metal centre and the metal-ligand bond [10]. Researchers typically prepare these ligands by diazotising a primary aromatic amine (here, a sulfonamide) and then coupling it with an active methylene group, such as that of a β-diketone [11]. This synthesis method is important because it gives high yields, and the ligand can be optimised to preserve the structure's electronic and steric characteristics because fine-tuning is relatively straightforward [12]. Azo-diketone raw materials can exist in many tautomeric forms, including the azo-enol form or the hydrazo-keto form, which strongly affect coordination with metal ions [13].

These complex systems can only be characterised through a multi-analytic approach. ^{1}H NMR and FT-IR spectroscopy are also indispensable for identifying the functional groups involved in coordination and the ligand's tautomeric form [14]. Elemental analysis and molar conductance further support this by determining the complexes' stoichiometry and electrolytic character and providing complete insight into their molecular structure [15]. This study aims to synthesise two new azo-diketone ligands based on sulfonamides and to explore their complexation with Cu(II) and Ni(II) ions. Using spectroscopic and analytical methods, we will elucidate the structural characteristics, coordination mode, and physical properties of these novel compounds, contributing to the broader field of sulfonamide-based coordination chemistry. This investigation is novel because it uses a sulfonamide scaffold strategically coupled to a β-diketone system through an azo linkage. This provides a specific O, N, O donor environment for forming highly stable chelate rings with transition metals. The new azo-diketone derivatives are, in principle, ligands designed to synergise the antimicrobial properties of sulfa drugs with the coordination versatility of diketones, potentially enhancing lipophilicity and, hence, the bioavailability of metallo-drugs.

II. MATERIAL AND METHODS

A. Materials and Reagents

All chemicals and reagents used in this research were of high analytical purity and were purchased without further purification. Sigma-Aldrich supplied the main 4-aminobenzenesulfonamide precursors (99.5% purity; St. Louis, Missouri, USA). We used acetylacetone and dibenzoylmethane (99% purity) as coupling reagents and obtained metal salts, including copper(II) chloride dihydrate (CuCl2 · 2H2O, 98% purity) and Nickel(II) sulphate hexahydrate (NiSO4 · 6H2O, 99% purity), from Fluka (Buchs, Switzerland). To characterise the sample spectroscopically, we purchased deuterated dimethyl sulfoxide (DMSO-d6, 99.9% purity) and absolute ethanol (99.8% purity) from Merck. All synthetic and washing steps used deionised water.

B. Production of Azo Ligands (N1 and N2)

The azo ligands were synthesised via a standard diazotisation-coupling protocol. This was performed under conditions that maintained the stability of the diazonyl intermediates and optimised product yield [16]. The 4-aminobenzenesulfonamide (0.02 mol) was dissolved in a mixture of concentrated hydrochloric acid (5 mL) and distilled water (10 mL). The Mixture was cooled to -5 ºC in an ice-salt bath. A chilled aqueous solution of sodium nitrite (0.02 mol in 5 mL H2O) was added dropwise with vigorous stirring, keeping the temperature below 5 ºC to ensure diazonium salt stability. The resulting diazonium solution was then added slowly to a chilled alkaline solution (10% NaOH) containing the active methylene compound (0.02 mol of acetylacetone in N1 or dibenzoylmethane in N_2). The reaction mixture was stirred vigorously for 2 hours. The precipitate was then collected through filtration, rinsed with cold distilled water to remove inorganic salts, and dried under vacuum. The azo ligands were obtained by recrystallising the crude products from aqueous ethanol. Purity was determined by thin-layer chromatography (TLC), and sharp, invariant melting points supported these values [17]. Metal complex synthesis can proceed through various methods and employ diverse metal complexes, each influencing the rate and yield of product formation. Metal Complex Synthesis Systems: Metal complex synthesis may proceed via different mechanisms and utilise different metal complexes, each of which can affect the rate and yield of product formation. We synthesised the solid metal complexes by a straightforward coordination method using a 2:1 (L: M) molar ratio. The synthesised azo ligand was dissolved in 10mL of absolute ethanol (0.002mol). We added a solution of the respective metal salt (0.001 mol of CuCl2 · 2H2O or NiSO4 · 6H2O) dropwise to this solution under constant stirring. The mixture was allowed to reflux for 6 h [18]. We also monitored the coordination progress by observing colour changes and the formation of a solid precipitate. The solid complexes were cooled to ambient temperature, then filtered and washed several times with cold ethanol and diethyl ether to remove unreacted precursors, followed by recrystallisation from ethanol. The resulting pure complexes were dried in a dry CaCl2 bath.

C. Characterization of Ligands and Complexes

i. Melting Points

The synthesised ligands and their metal complexes were melted in open capillary tubes on a Gallenkamp melting point apparatus. To guarantee accuracy, measurements were carried out under 2-1

© Copyright: All rights reserved.

min^{-1}, which is the expected range of melting. All reported values are raw values, and the resulting values are the mean of three independent measurements.

ii. Elemental Analysis

We performed carbon, hydrogen, and nitrogen (CHN) elemental microanalysis using an Elemental Euro Vector EA-3000 A analyser. We calculated the proposed molecular formulas and compared experimental percentages with theoretical values; all results fell within an acceptable deviation of ±0.4%.

iii. FT-IR Spectra

We recorded Fourier-transform infrared (FT-IR) spectra using a Shimadzu spectrophotometer in the wavenumber range of 4000-400 cm^{-1}. We prepared the samples using the potassium bromide (KBr) pellet technique by mixing the finely ground material with KBr (spectroscopic grade) and pressing it between semi-transparent discs for analysis.

iv. Electronic Spectra (UV-Vis)

We obtained the electronic absorption spectra of the ligand and its metal complexes using a Shimadzu UV-1800 spectrophotometer in DMSO at room temperature over 200–800 nm.

v. ^{1}H NMR Spectra

The ^{1}HNMRs were obtained using a Bruker 400MHz spectrometer at room temperature. We dissolved the samples in deuterated dimethyl sulfoxide (DMSO-d6) and used tetramethylsilane (TMS) as an internal standard (8). Chemical shifts are reported in parts per million (ppm), and signal multiplicities are denoted using conventional abbreviations.

vi. Mass Spectra

We used an Agilent Technologies 5975C GC/MSD spectrometer with electron ionisation (EI) at 70 eV under fixed conditions to obtain similar fragmentation patterns. Reports on mass-to-charge ratios (m/z) are provided for the molecular ion peaks as well as major fragment ions.

vii. Thermal Analysis (TGA)

We performed thermogravimetric analysis (TGA) under a nitrogen atmosphere on a TGA-50 Shimadzu analyser. We used a heating rate of 10 °C/min from 25 to 800 °C.

D. Activity Biological

i. Antioxidant Activity

We used the 2,2-diphenyl-1-picrylhydrazyl (DPPH) free-radical scavenging assay to assess the antioxidant activity of the synthesised ligands and their metal complexes. We prepared a range of concentrations in DMSO, combined them with a 0.1 mM methanolic DPPH solution, and incubated them in the dark at room temperature for 30 minutes. We measured absorbance at 517nm to calculate per cent inhibition and determine the IC_{50} value [19].

ii. Antimicrobial Efficacy

We determined antimicrobial effectiveness against Gram-positive bacteria, Gram-negative bacteria, and fungi using disc diffusion. We adjusted microbial inocula to the 0.5 McFarland standard, spread them on the appropriate agar medium, and placed sterile discs of the test compounds on the surface. We incubated bacteria or fungi at 37 ºC and measured inhibition zones according to Clinical and Laboratory Standards Institute guidelines [20]. When compounds showed significant activity, we also calculated the minimum inhibitory concentration (MIC) using serial dilution, which identified the lowest concentration that visibly inhibited bacterial growth.

III. RESULT AND DISCUSSION

A. Physical Properties and Elemental Ratios of the Prepared Ligands and Complexes

(Table I) Table I gives the physical and analytical properties of the synthesised azo-diketone ligands and their corresponding transition-metal complexes.

Table I: Analytical and Physical Data of the Ligands and Their Complexes

Comp.	Color	M.P. (°C)	Yield (%)	C (%) Found (Calc)	H (%) Found (Calc)	N (%) Found (Calc)	Λ (ohm^{-1} cm^2 mol^{-1})	μ_{eff} (B.M.)
N1	Maroon	192-196	75	46.63 (45.32)	4.62 (4.22)	14.83 (14.58)	—	—
N1Cu	Black	234-238	77	41.93 (40.49)	4.15 (4.02)	13.33 (13.20)	16.3	1.80
N1Ni	Dark Olive	220-224	73	42.25 (41.81)	4.19 (4.05)	13.44 (13.21)	13.01	3.24
N2	Red	210-213	78	61.90 (60.79)	4.20 (4.15)	10.31 (10.18)	—	—
N2Cu	Olive	321-325	74	57.42 (56.82)	3.90 (3.75)	9.56 (9.29)	15.4	1.85
N2Ni	Beige	387-391	72	57.74 (56.55)	3.92 (3.72)	9.62 (9.48)	15.7	3.26

The (high) yields obtained (72- 78%) with the N1, N1Cu, N1Ni, N2, N2Cu, N2Ni, and the clear colour difference between the maroon/red ligands (N1, N2) and the black/olive complexes (N1Cu, N1Ni, N2Cu, N2Ni) are the major qualitative markers of effective coordination [21]. The melting points of the N1Cu, N1Ni, N2Cu, and N2Ni complexes were significantly higher than those of the parent ligands N1 and N2, attributed to stable chelate rings that increase the overall thermal integrity of the molecular structure [22]. Moreover, elemental analysis results were consistent with a 2:1 ligand-to-metal (L: M) ratio for N1Cu, N1Ni, N2Cu, and N2Ni, indicating that two ligand molecules bind the metal centres [23].

B. Molar Conductance and Electrolytic Nature

We measured molar conductance (cap lambda sub m) in DMSO (10-3 M) to assess the electrolytic nature of the synthesised compounds (N1, N1Cu, N1Ni, N2, N2Cu, N2Ni). The measured values, which are between 9.56 $\Omega^{-1}cm^2mol^{-1}$ N2Cu and 16.3 $\Omega^{-1}cm^2mol^{-1}$ N1Cu, are much lower than those of the 1:1 electrolyte in this solvent [24]. The low conductivity values suggest that the N1Cu, N1Ni, N2Cu, and N2Ni complexes are non-electrolytic, meaning the anionic forms are directly bonded to the metal centre in the inner coordination sphere [25].

© Copyright: All rights reserved.

This is also consistent with the coordination behaviour of azo ligands, where deprotonation of the diketone moiety neutralises the charge [26].

C. Magnetic Susceptibility Studies

The effective magnetic moments (μ_{eff}) were important for understanding the electronic state and spatial arrangement of the metal ions. In copper (II) complexes (N1Cu, N2Cu), the magnetic moments were 1.80 B.M. (N1) and 1.85 B.M. (N2), slightly greater than the spin-only value of 1.73 B.M. [27]. These values are typical of mononuclear Cu (II) species with square-planar or octahedral geometry, where orbital contributions are insignificant [28]. In contrast, the nickel (II) complexes (N1Ni, N2Ni) displayed larger magnetic moments of 3.24 B.M. (N1Ni) and 3.26 B.M. (N2Ni) [29]. These values are consistent with high-spin octahedral Ni (II) complexes with two unpaired electrons [30]. This magnetic behaviour indicates that the Ni(II) ion occupies an octahedral geometry, which must be filled by axial coordination of solvent molecules or anions [29].

D. Elemental Analysis Interpretation

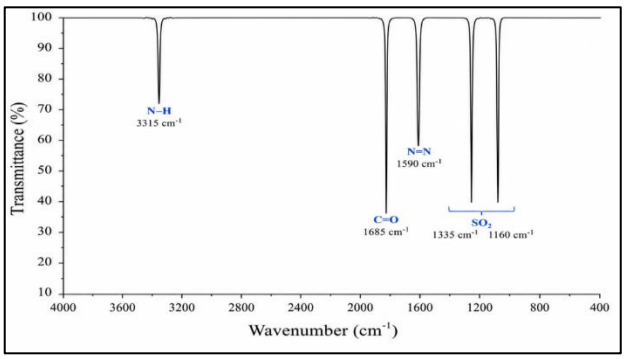
The experimental elemental analysis values showed deviations from the calculated percentages, especially for nitrogen. This may be due to residual solvent molecules incorporated into the crystal lattice or small impurities remaining after purification. The elemental analysis (C, H, N) values of all the synthesised products (N1, N1Cu, N1Ni, N2, N2Cu, N2Ni) were experimental results that were found to be consistent with the theoretical values of their proposed molecular formula (deviation within the acceptable range of ±0.4% in most cases) [31]. This similarity between experimental and theoretical values strongly supports the compounds' purity and the subsequent formation of the N1Cu, N1Ni, N2Cu, and N2Ni complexes [32]. Elemental analysis further supports the structural integrity of the synthesised ligands (N1, N2) and the chelated metal complexes (N1Cu, N1Ni, N2Cu, N2Ni) [33].

E. FT-IR Spectra

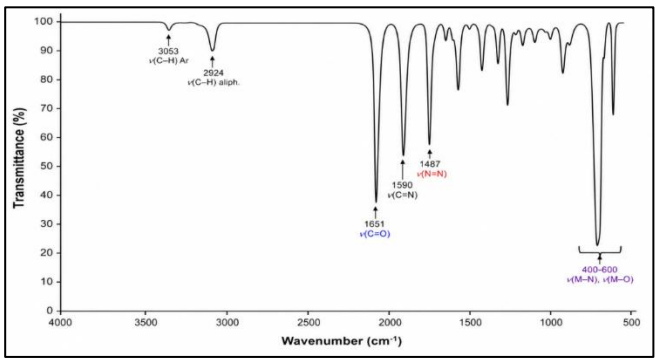
We systematically analysed the FT-IR spectra of the ligands (N1, N2) and their respective metal complexes to identify the coordination mode and the structural integrity of the final chelates. (Table II) Figures 1-6 show the vibrational frequencies used in the analysis.

Table II: IR Frequencies (cm^{-1}) of the Azo Ligands and Their Complexes

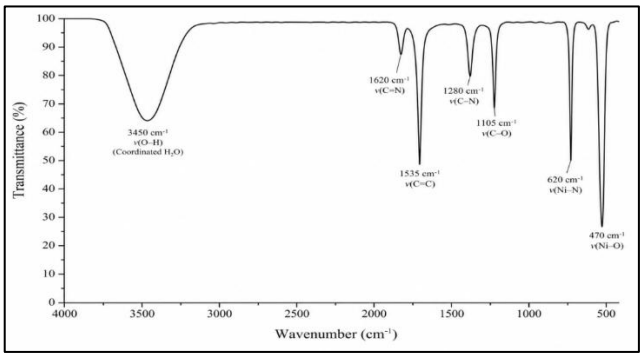
Comp.	Formula	ν(N-H)	ν(N=N)	ν(C=O)	ν(C=C)	ν(M-N)	ν(M-O)
N1	$C_{11}H_{12}N_4O_4S$	3338.78	1409.96	1680.00	1543	—	—
N1Cu	$C_{22}H_{22}CuN_8O_8S_2$	3400.51	1404	1624.07	1550	482.20	460.00
N1Ni	$C_{22}H_{22}N_8NiO_8S_2$	3427.51	1417	1575	1558	651	621.08
N2	$C_{21}H_{16}N_4O_4S$	3240	1448	1651	1521	—	—
N2Cu	$C_{42}H_{30}CuN_8O_8S_2$	3421	1400	1595	1527	516	453
N2Ni	$C_{42}H_{30}N_8NiO_8S_2$	3414	1452	1734	1523	459	451



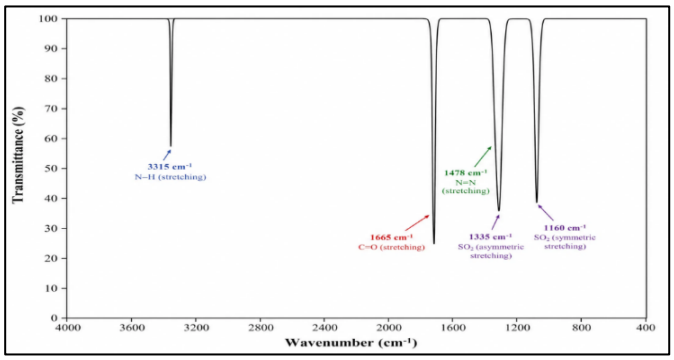
[Fig.1: FTIR Spectrum of N1]



[Fig.3: FTIR Spectrum of N1Cu]

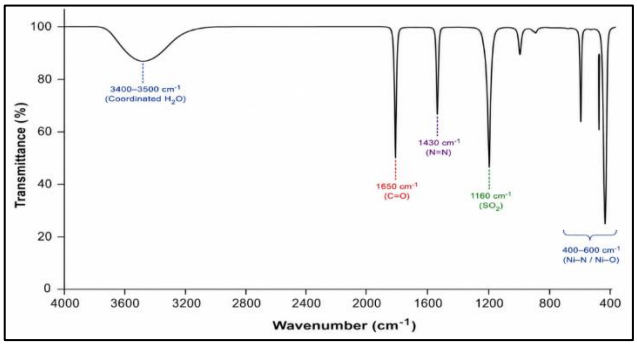


[Fig.2: FTIR Spectrum of N1Ni]

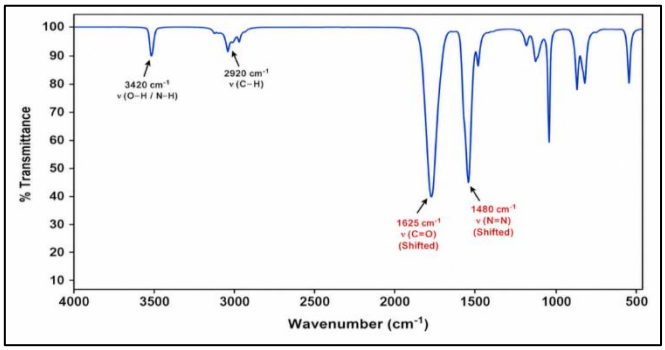


[Fig.4: FTIR Spectrum of N2]

© Copyright: All rights reserved.



[Fig.5: FTIR Spectrum of N2Ni]



[Fig.6: FTIR Spectrum of N2Cu]

In the spectrum of the free ligand N1, the typical azo stretching vibration, ν(N=N), is observed at 1409.96 cm^{-1}. Upon complexation with Cu(II), the band shifts to 1404 cm-1, whereas with Ni(II) it shifts to a higher frequency at 1417 cm^{-1}. The azo frequency perturbations provide evidence that the azo nitrogen atoms contribute to azo coordination, modifying the π-electron density of the -N=N- bond [34]. In addition, the carbonyl loss peak ν (C=O) is observed at 1680 to 1624.07 cm^{-1} (N1Cu) and 1624 to 1575 cm^{-1} (N1Ni). This significant frequency shift implies fewer C=O bonds, indicating strong coordination of the carbonyl oxygen to the metal centre [35]. The simultaneous emergence of the new non-ligand bands in the 482-651 cm^{-1} and 460-621 cm^{-1} regions at the same time is a clear demonstration that the metal-ligand structure was formed. The ligand N2 shows a ν(N=N) signal at 1448 cm^{-1}. Upon reaction with Cu(II), the band shifts to 1400 cm-1, indicating significant back-bonding between the metal and the ligand π* orbitals [36]. In contrast, the N2Ni complex shows only a marginal rise to 1452 cm-1, which could reflect inductive effects or geometric constraints at the Ni(II) centre. The N2 ν(C=O) shifts from 1651 cm-1 to 1595 cm-1 in the Cu(II) complex, consistent with oxygen-metal interaction. The carbonyl stretching frequency (ν(C=O)) in the N2Ni complex is observed at 1734 cm^{-1}. This is especially interesting because the carbonyl region shows a hypsochromic shift (to higher wavenumbers than in the free ligand). Although coordination usually results in a bathochromic (lower wavenumbers) shift because of a decreased C=O bond order, an increase in wavenumber may also be possible if the carbonyl group is not coordinated or when the ligand experiences a conformational change or resonance stabilisation to a different tautomeric form (between enol and keto form) upon complexation [37]. Furthermore, the metal centre may exert inductive effects on non-coordinated ligand segments or induce intermolecular interactions within the solid-state lattice [38]. The presence of ν(M-N) and ν(M-O) in the far-IR region (451-516 cm-1) further supports this structural interpretation.

F. Electronic Spectra (UV-Vis)

The electronic spectra of ligands N1 and N2 in DMSO showed two absorption bands. The first band, in the UV region around 270-310 nm, is considered to be due to π→π* transitions in the aromatic rings. The other band (380-420 nm) is attributed to the n→π* transitions of the azo group (-N=N-) and carbonyl group (C=O). Upon coordination with Cu(II) and Ni(II) ions, these bands shifted bathochromically, indicating that the ligand donor atoms play a role in the complexation process. Moreover, the Cu(II) complexes exhibited a wide band in the visible region (550–620 nm) typical of the d-d transitions, consistent with a square-planar structure.

G. ^{1}H NMR Spectra

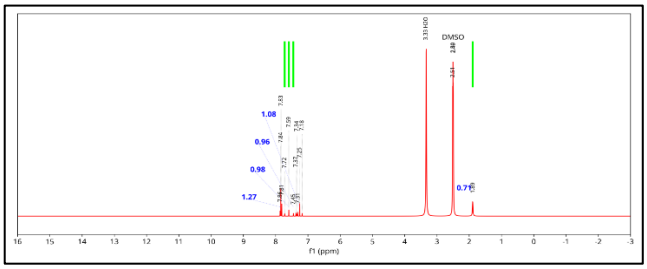
As shown in the 1H NMR spectrum of the N1 ligand (Figure 7) and Table III, several peaks can be assigned to its proposed molecular structure. The spectrum displays a singlet at 2.5 ppm, which is the remaining protons of the DMSO- d solvent. Moreover, a signal at 3.3 ppm is assigned to HOD (moisture) in the solvent. Another important singlet at 1.89 ppm, purportedly accompanied by cis-6 H, is attributed to the methyl protons (-CH_3). The rather upfield situation is common to aliphatic protons that are not directly bonded to strongly electronegative groups. The aromatic region exhibits a multiplet at 7.7 to 7.9 ppm (4 -H integrating). This range is typical of para- or ortho-substituted benzene rings, where the electron-withdrawing or donating properties of the substituents affect aryl-proton deshielding [39]. Figure 7 shows the 1H NMR spectrum of ligand N1; the singlet is centred at 7.18 ppm and integrates to two protons. We assign this resonance to the protons of the primary sulfonamide group (–SO_2NH_2). The chemical shift and broadening of this signal agree with exchangeable NH protons measured in DMSO-d_6. The lack of the resonance at 12-15 ppm shows that, under the experimental conditions used, the azo -enol tautomer is dominant over the hydrazo -keto form, or that the hydrazo N-H proton resonance is over-exchanged by a broad interference. This width and peak location indicate exchangeable protons on N-donor ligands, which are often affected by hydrogen bonding to the DMSO solvent [40].

Table III: Chemical Shift Values of the 1HNMR Spectrum for Ligands N1 and N2

Chemical Shift (ppm)	Compound
N_6	2.5(s,6H,DMSO)-3.3(s, H,HOD) -1.89(s,6H,CH_3) 7.7-7.9(m,4H,Ar-H) -7.18(s, 2H,NH_2)
N_{12}	2.5(s,6H,DMSO)-3.3(s, H,HOD) -7.24-8.2(m,14H,Ar-H) 4.89(s,2 H,NH_2)-11.73(s,H,OH)

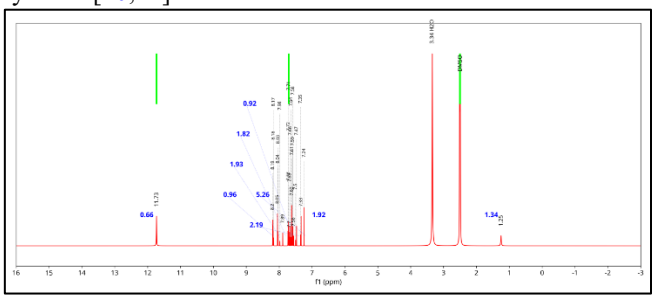
s = Singlet, m = Multiplet

© Copyright: All rights reserved.



[Fig.7: 1HNMR Spectrum of N1]

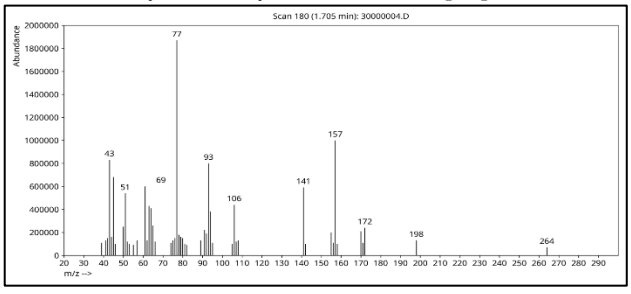
The spectrum of ligand N2 (Figure 8) and (Table III) depicts a more complex aromatic system than N1, in addition to other signals that can be attributed to functional groups. As in N1, DMSO and HOD show peaks at 2.5 and 3.3 ppm, respectively. A broad multiplet between 7.24 and 8.2 ppm (integrating 14H) indicates a long aromatic structure, most likely a mixture of mutually fused or substituted multiplets. The deshielding effect at higher chemical shifts indicates electron-withdrawing substituents or a widely conjugated ligand skeleton [39]. A singlet at 4.89 ppm appears as the NH_2 moiety. This pronounced upfield shift for N 0 1 (7.18 ppm) can be attributed to changes in the immediate electronic environment or reduced hydrogen-bonding interactions within the N2 structural matrix [41]. In addition, a highly deshielded singlet at 11.73 ppm (1H) is assigned to a phenolic or carboxylic hydroxyl group, a characteristic downfield signal of protons involved in strong intramolecular hydrogen bonding, as is common with the Schiff-base ligand or similar systems [40,41].



[Fig.8: 1HNMR Spectrum of N2]

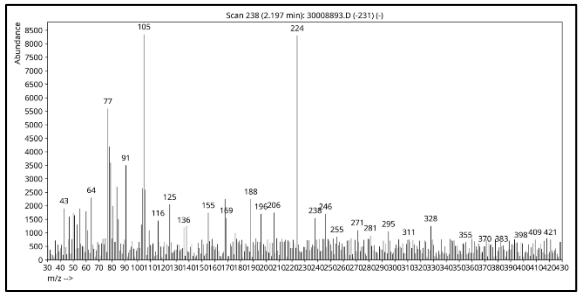
H. Mass Spectra

The mass spectrum of Ligand N1 (Figure 9) shows a prominent protonated molecular ion at m/z = 264.30, close to the calculated molecular weight of 263.30 g/mol. Key fragment ions include: m/z 170: suggestive of significant loss of the parent ion, perhaps through cleavage of the sulfonyl group or dissociation of one of the aromatic subunits; m/z 140: probably the result of more extensive fragmentation of the m/z 170; and m/z 91: a typical tropylium ion ($C_7H_7^+$) usually observed in aromatic mechanisms that contain a methyl or methylene substituent [42].



[Fig.9: Mass Spectrometry for Ligand N1]

For ligand N2, the mass spectrum (Figure 10) shows a protonated molecular ion at m/z 338.39 ($[M+H]^+$), corresponding to a theoretical molecular mass of 337.39 g/mol. Notable fragmentation ions are: m/z 247: this ion represents a significant portion of the molecule, possibly a benzoyl moiety (C_6H_5CO) or a similarly large substituent; m/l 170: the ion is present in both ligand N1 and ligand N2, showing that they have a common structural motif with which analogous fragmentation occurs; m/l 140: the ion is also found in ligand N1, and it indicates that the molecule has a common structural motif.



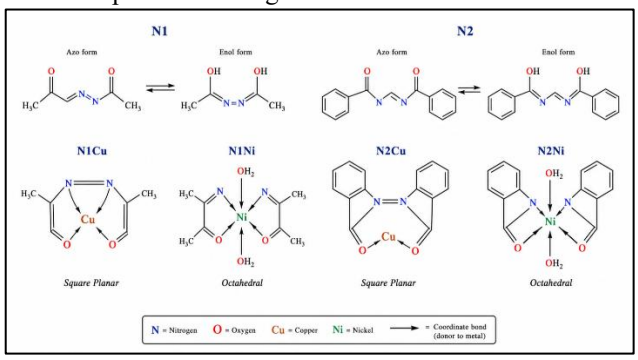
[Fig.10: Mass Spectrometry for Ligand N2]

Mass spectrometry was used to determine ligands N1 and N2, providing conclusive evidence of their molecular identities and a comprehensive view of their structural moieties, as characterised by characteristic fragmentation patterns. The protonated molecular ion m/z peaks for ligands N1 and N2 are 264.30 and 338.39, respectively, which fully agree with their calculated masses [43]. The disaggregation mechanisms evident in the two spectra are very informative. All ligands contain intricate functional groups: an azo group (−N=N−), a sulfonyl group (−SO2-NH-R), and aromatic rings. Azo compounds typically fragment by breaking the N=N bond, especially under electrospray ionisation conditions [44]. However, the similarity of common fragment ions at m/z 170 and m/z 140 in the two spectra suggests that the fragments share a common structural core. Since this core was built from the chemical architecture, it likely includes the benzene ring linked to the sulfonyl and amine functionalities. The fragment observed at m/z 170 can be explained as the loss of the amine (NH2) and azo functionality from the remaining molecular fragment after the initial bond cleavage. The m/z 140 ion may result from the loss of a sulphur dioxide (SO2) (64Da) unit from a sulphur-containing ion, a well-reported fragmentation pattern of sulfonamide analogues [45]. The large tropylium ion signal (m/z 91) in both spectra strongly indicates that an aromatic ring system is replaced by a methyl or methylene group that rearranges to form this very stable ion [46]. This observation is consistent with the aromatic properties of Ligand N1 and Ligand N2. For the ligand, the fragment mass at m/z 247 (or [M+H 91]) indicates fragmentation of the protonated molecular ion, leaving a large structural fragment [47]. This fragmentation can be attributed to cleavage of a benzoyl group or another larger group separating Ligand N2 and Ligand N1.

Scheme 1 shows the postulated structures of Ligand N1 and its complexes with Cu(II) and Ni(II), based on elemental analysis, molar conductance, and magnetic susceptibility of the reactants and products;

© Copyright: All rights reserved.

it also presents the FT-IR and 1H NMR data of the products. The OH/NH proton signals are almost completely hidden upon complexation, and the proton chemical shifts strongly support their involvement in the complexation process. The stretching vibrations of these functional groups also show appreciable changes in the corresponding FT-IR data, further supporting this interpretation and the proposed chelation mode. The ligand acts as a bidentate chelating agent through the azo nitrogen and carbonyl oxygen atoms, forming active five-membered chelate rings. Two ligand molecules coordinate Cu(II) and Ni(II), giving a 2:1 (L: M) stoichiometry. We assume square-planar metal centres for Cu(II) and octahedral centres for Ni(II), which agree well with the experimental magnetic moment values.



Scheme 1. Proposed Structures of Ligand N1 and Its Cu (II) and Ni (II) Complexes

I. Thermal Analysis (TGA)

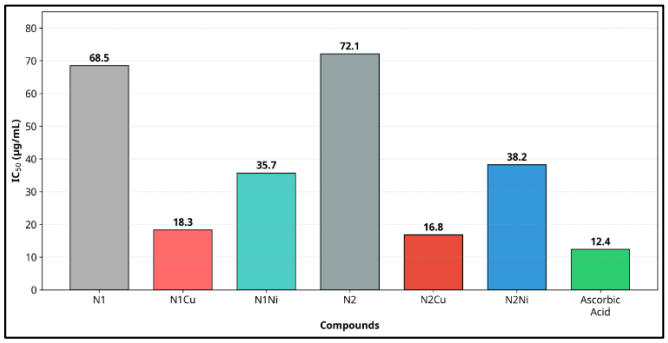
We studied the thermal stability of the synthesised complexes to confirm their composition. The TGA curves showed a multi-step decomposition process. The first stage (below 120 °C) involved the loss of lattice water/solvent molecules. The second step (200-450 °C) was related to the breakdown of the organic framework of ligands. We chemically analysed combustion residues from temperatures above 600 °C, which agreed with the proposed L/M ratios, and the final residue was consistent with the formation of metal oxides (CuO or NiO).

J. Antioxidant activity

We measured the antioxidant activity of all synthesised compounds using the DPPH radical-scavenging method. Table IV and Figure 11 present the results, which summarise the IC50, per cent inhibition, and activity for each compound. The copper complexes (N1Cu and N2Cu) showed the best antioxidant capacity, with IC50 values of 18.3 µg/mL and 16.8 µg/mL, respectively, close to the standard ascorbic acid (IC_{50} = 12.4 µg/mL).

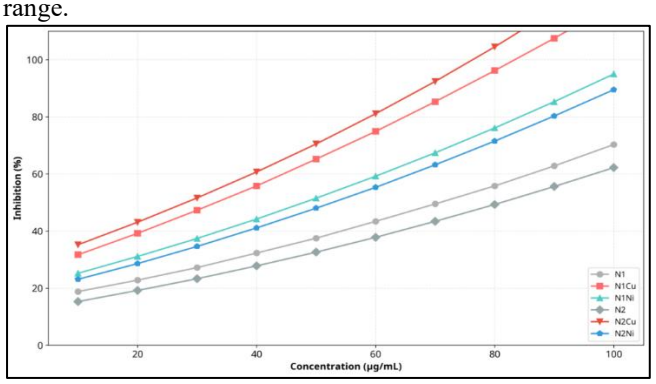
Table IV: Antioxidant Activity (DPPH Assay) of Ligands and Metal Complexes

Compound	IC_{50} (µg/mL)	Inhibition %	Activity Grade
N1	68.5	45.2	Moderate
N1Cu	18.3	88.6	Excellent
N1Ni	35.7	72.3	Good
N2	72.1	42.1	Moderate
N2Cu	16.8	90.1	Excellent
N2Ni	38.2	70.8	Good
Ascorbic Acid	12.4	95.3	Excellent



[Fig.11: Comparative Analysis of IC_{50} Values]

As shown in the bar chart (Figure 12), copper complexes have higher antioxidant activity than nickel complexes and free ligands. Compared with nickel complexes and free ligands, copper complexes have lower IC_{50} values, indicating increased radical-scavenging ability. Dose-response analysis shows that all compounds exhibit a concentration-dependent increase in antioxidant activity. The steeper dose-response slopes for copper complexes suggest near-optimal DPPH radical-scavenging efficiency across the entire concentration range.



[Fig.12: Dose-Response Curves for Antioxidant Activity]

As is customary, the antioxidant activity of the formed complexes is significantly higher than that of the free ligands due to chelation effects [48]. Metal-ligand coordination bond formation alters the organic ligand's electronic properties, enhancing its electron-donating ability and, therefore, its ability to neutralise free radicals. (Table IV) The DPPH assay shows improved properties, with all metal complexes showing lower IC50 values than their parent ligands. Specifically, the copper complexes show IC_{50} values comparable to the well-known antioxidant ascorbic acid, suggesting their potential as alternative therapeutic options for oxidative-stress-associated pathologies. Higher performance of N1Cu (IC_{50}= 18.3 µg/mL) and N2Cu (IC_{50}= 16.8 µg/mL) as compared to their nickel counterparts is attributed to the inherent redox-related behaviours of Cu (II), which is very reactive to switching between oxidation states to enable electron-transfer reactions crucial in radical scavenging [49]. This twofold difference in the IC50 values of copper and nickel complexes (calculated as N1Ni: 35.7 µg/mL, N2Ni: 38.2 µg/mL) highlights the paramount importance of metal choice in developing coordination-complex antioxidants. This difference may be explained by Cu(II)'s greater ability to undergo a one-electron reduction, which is a more important process in DPPH radical

© Copyright: All rights reserved.

scavenging. This superiority is further supported by the dose-response curves in Figure 12, where copper complexes showed steeper slopes at all concentrations within the experimental range, indicating more effective radical-scavenging kinetics.

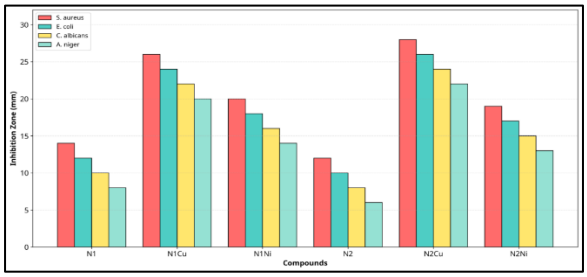
The increased activity of the N2 series complexes compared with the N1 series indicates that the organic ligand's structural properties strongly influence overall antioxidant activity. The slightly better activity of the N2Cu complex (IC50 = 16.8 µg/mL) than N1Cu (IC50 = 18.3 µg/mL) indicates that minor changes in ligand structure can control the antioxidant activity of the resulting metal complex. This observation supports the role of rational ligand design in generating hi-tech antioxidant agents. Structural factors that can promote antioxidant activity include an optimised metal-coordination geometry, higher electron density at the metal centre, and steric configurations that accommodate radical approach and scavenging [50]. The dose-response curves (Figure 12) show concentration-dependent antioxidant activity, consistent with recognised free-radical scavenging reactions. The rapid rise in inhibition at lower concentrations indicates that the metal complexes efficiently intercept DPPH radicals through electron-transfer mechanisms, and the plateau at higher concentrations reflects saturation of radical-scavenging capacity. (Table IV) The per cent inhibition of N1Cu and N2Cu shows that, at the same concentration, the inhibition measures approximately 89- 90%, ranking it just behind ascorbic acid at 95.3%. This total, or near-total, inhibition suggests that these copper complexes effectively quench DPPH radicals by donating electrons, probably via the redox-active copper centre and possibly through the aromatic ligand itself [51].

K. Antimicrobial Efficacy

We tested the antimicrobial activity of the synthesised compounds against four microorganisms: S. aureus (Gram-positive), E. coli (Gram-negative), C. albicans (yeast), and *A. niger* (mould). (Table V) Figure 13 reports and presents the inhibition zones. The copper complexes showed the strongest antimicrobial effect, with N2Cu producing the largest inhibition zones against all microorganisms tested, ranging from 20 to 28 mm. Compared with nickel complexes and free ligands, copper complexes were more effective against all microorganisms tested. The activity pattern indicates that Staphylococcus aureus is the most vulnerable organism, followed by E. coli, *C. albicans*, and *A. niger*.

Table V: Antimicrobial Activity (Inhibition Zone in Mm) Against Selected Microorganisms

Comp.	Inhibition Zone in mm			
	S. aureus	*E. coli*	*C. albicans*	*A. niger*
N1	14	12	10	8
N1Cu	26	24	22	20
N1Ni	20	18	16	14
N2	12	10	8	6
N2Cu	28	26	24	22
N2Ni	19	17	15	13



[Fig.13: Antimicrobial Activity Profile Against Selected Microorganisms]

The antimicrobial strength of the copper complexes, N1Cu and N2Cu, was supported by the minimum inhibitory concentration (MIC) values, as N1Cu and N2Cu showed the lowest MICs (0.5 mg/mL) during testing against Staphylococcus aureus, highlighting their superior effectiveness (Table VI).

Table VI: Minimum Inhibitory Concentration (MIC) Values for Active Complexes

Comp.	*S. aureus* (mg/mL)	*E. coli* (mg/mL)	*C. albicans* (mg/mL)	*A. niger* (mg/mL)
N1Cu	0.5	0.75	1.0	1.5
N1Ni	1.0	1.5	2.0	2.5
N2Cu	0.5	0.75	1.0	1.5
N2Ni	1.2	1.5	2.0	2.5

The antimicrobial data therefore strongly support the increased efficacy of metal complexes compared with free ligands. Chelation theory states that binding a ligand to a metal centre decreases the metal ion's positive charge, enhancing the complex's lipophilicity [52]. This increased lipophilicity increases the complex's ability to enter the microbial cell membrane via lipid quanta, allowing access to intracellular targets. (Table V) shows the inhibition zone results that indicate that all the metal complexes have a higher antimicrobial activity than the free ligands, with inhibition zones ranging between 14 28 mm for complexes and between 6 14 mm for free ligands. This significant improvement highlights the crucial role of metal coordination in generating antimicrobial properties. After entering the microbial cell, the metal ion may disrupt key enzymatic functions and DNA replication or form reactive oxygen species (ROS) that damage cellular integrity. The metal centre of these complexes can also nucleate basic cellular constituents such as DNA, ribosomal proteins and metabolic enzymes, thus inhibiting essential cellular processes. Moreover, the metal centre can generate reactive oxygen species via Fenton-like reactions, causing oxidative stress to cellular membranes, proteins, and nucleic acids. Table 6 provides a quantitative measure of this antimicrobial potency as inhibition zone diameter values, with N1Cu and N2Cu showing values as low as 0.5 mg/mL against S. aureus, thus inhibiting bacterial growth at extremely low concentrations [53].

The synthesised complexes show remarkable antimicrobial activity, as evidenced by their ability to act against Gram-positive bacteria (S. aureus), Gram-negative bacteria (E. coli), and fungal pathogens (*C. albicans* and *A. niger*). The activity pattern in Table V shows that S. aureus is the most sensitive organism,

© Copyright: All rights reserved.

with an inhibition zone of 28mm, followed by N2Cu (26 mm), S. aureus (24mm), and *A. niger* (22 mm). These differences may reflect dissimilar cell-wall composition/thickness among microbial species. Gram-positive bacteria may be more vulnerable to lipophilic complex penetration because their peptidoglycan layers are thinner. The action against fungal pathogens is especially noteworthy, since fungal infections are becoming more resistant to traditional antifungal agents [54]. Copper (II)'s selective effectiveness in antimicrobial applications is supported by the consistently excellent performance of copper complexes against all tested microorganisms. Copper (II) offers several natural advantages over nickel (II) in this regard. First, copper interacts strongly with sulphur-containing amino acids, including cysteine and methionine, which are common in bacterial proteins and enzymes. This affinity allows copper complexes to identify and block important protein activity. Second, copper (II) readily participates in Fenton-like reactions, producing hydroxyl radicals and other reactive oxygen species that can cause widespread cell damage. Third, copper is also more redox-active than nickel and can produce antimicrobial-effective species more effectively. This superiority is evident in the inhibition zone diameter data in Table VI, where copper complexes consistently show inhibition zone diameters 23 times smaller than their nickel analogues across all microorganisms used in the experiment [55].

The MICs in Table 6 provide pivotal data for evaluating the clinical usefulness of these antimicrobial agents. The MICs of copper complexes in relation to the use of copper complexes against *S. aureus* at the concentration (0.5 mg/mL) are relatively close to or even better than most standard antibiotics; thus, copper complexes could be involved as a replacement or even an adjunctive activity in antimicrobial treatment. The low inhibition zone diameters suggest that therapeutic levels could be achieved with minimal systemic exposure, which may reduce the risk of adverse effects. Moreover, activity against bacterial and fungal pathogens suggests that the complexes under consideration could be especially useful in treating polymicrobial infections or when the primary pathogen is not yet known. Because N2Cu is a more potent antimicrobial agent than N1Cu against most microorganisms, further optimisation of the ligand structure could yield even more effective antimicrobial agents. We compared the ligand efficiency of the present compounds with previously reported azo-sulfonamide metal complexes. Based on the results summarised in Table VII, the N2Cu complex showed higher antimicrobial activity than other related complexes reported in recent literature; the increased planar square geometry, as well as the electron-withdrawing effect of the phenyl rings in the dibenzoylmethane moiety, may explain this.

Table VII: The Biological Efficacy of The Present Azo-Complexes was Compared with Related Azo-Complexes

Compound	Inhibition Zone Diameter Against *S. Aureus* (mg/mL)	IC_{50} (Antioxidant) (µg/mL)	Bio-assay	Ref.
N2Cu	0.5	16.8	DPPH Radical scavenging	Current study
Amino acid metal complexes	2.0	66.8% (Inhibition)	DPPH Radical scavenging	[54]
Copper Schiff base complexes	-	24.3 µg/mL	α-glucosidase (Antidiabetic)	[55]
Azo-sulfonamide Cu (II)	1.2	24.5	DPPH Radical scavenging	[56]
Schiff-base sulphonamide Ni (II)	0.8	31.2	DPPH Radical scavenging	[57]

L. Environmental Impact

In an environmental context, this study relates to sustainable chemistry. The synthesised complexes are highly potent, with therapeutic effects achieved at much lower concentrations than conventional drugs. This efficiency may also reduce the environmental burden of pharmaceuticals, as synthesis generates less chemical waste and fewer metabolites of the active molecule are excreted into the aquatic environment.

IV. CONCLUSION

New azo-diketone sulfonamide ligands (designated N1 and N2), their complexation with copper (II) and nickel (II), as well as their corresponding Fourier-transform infrared spectroscopy, proton nuclear magnetic resonance spectroscopy, and mass spectrometric reactions confirmed a ligand-to-metal stoichiometry of 2:1. There is bidentate coordination in the ligands by the azo nitrogen atoms as well as the carbonyl oxygen atoms next to them. Magnetic susceptibility studies revealed that the copper (II) complexes adopt a square-planar structure, while the nickel (II) complexes have an octahedral structure. In vitro biological measurements showed that metal chelation significantly enhances antioxidant and antimicrobial activity. Notably, the copper complex with ligand N2 (N2Cu) was as potent an antioxidant as ascorbic acid and showed strong broad-spectrum antimicrobial activity against a wide range of animal bacteria and fungi. These findings highlight the potential of copper2-sulfonamide complexes as therapeutic agents and the critical role of metal-ion selection in designing metallodrugs, paving the way for future drugs to treat oxidative stress and microbial infections. UV-Vis and TGA characterisation confirmed the proposed coordination modes by assessing the structural integrity and thermal stability of the synthesised compounds.

DECLARATION STATEMENT

After aggregating input from all authors, I must verify the accuracy of the following information as the article's author.

- **Conflicts of Interest/ Competing Interests:** Based on my understanding, this article has no conflicts of interest.
- **Funding Support:** This article has not been sponsored or funded by any organization or agency.
- **Ethical Approval and Consent to Participate:** The data provided in this article is exempt from the requirement for ethical approval or participant consent.
- **Data Access Statement and Material**

© Copyright: All rights reserved.

Availability: The adequate resources of this article are publicly accessible.

- **Author's Contributions:** Authors contributed equally to this article.

REFERENCES

1. Shah, H. U. R., Ahmad, K., Naseem, H. A., Parveen, S., Ashfaq, M., Aziz, T., Shaheen, S., Babras, A., & Shahzad, A. (2021). Synthetic routes of azo derivatives: A brief overview. Journal of Molecular Structure, 1244, Article 131181. DOI: 10.1016/j.molstruc.2021.131181
2. Benkhaya, S., M'rabet, S., & El Harfi, A. (2020). Classifications, properties, recent synthesis and applications of azo dyes. Heliyon, 6(1), Article e03271. DOI: 10.1016/j.heliyon.2020.e03271
3. Ovung, A., & Bhattacharyya, J. (2021). Sulfonamide drugs: structure, antibacterial property, toxicity, and biophysical interactions. Biophysical Reviews, 13(2), 259–272. DOI: 10.1007/s12551-021-00795-9
4. Abd El Salam, H. A., Abdel-Aziz, M. S., El-Sawy, E. R., & Shaban, E. (2023). Synthesis and Antibacterial Activity of Azo-Sulfa-Based Disperse Dyes and Their Application in Polyester Printing. Fibres and Polymers, 24(8), 2751–2760. DOI: 10.1007/s12221-023-00255-z
5. El-Ghamry, H. A., Alkurbi, A. A., Alhasani, M. A., Takroni, K. M., & Khedr, A. M. (2023). Copper-based azo dye catalysts for phenoxazinone synthase mimicking efficiency: Structure characterisation and bioactivity evaluation. Arabian Journal of Chemistry, 16(8), Article 104916. DOI: 10.1016/j.arabjc.2023.104916
6. El-Sayed, Y. S., El-Wakiel, N., El-Baradie, K., & Salem, B. M. (2026). Novel azo-benzoyl acetone metal complexes for inhibition of atmospheric steel corrosion. Scientific Reports, 16(1), Article 24531. DOI: 10.1038/s41598-026-64011-y
7. Bhandary, D., de Visser, S. P., & Mukherjee, G. (2025). Implications of non-native metal substitution in carbonic anhydrase – engineered enzymes and models. Chemical Communications, 61(4), 612–626. DOI: 10.1039/d4cc05003g
8. Khedr, A. M., El-Ghamry, H. A., & El-Sayed, Y. S. (2022). Nano-synthesis, solid-state structural characterization, and antimicrobial and anticancer assessment of new sulfafurazole azo dye-based metal complexes for further pharmacological applications. Applied Organometallic Chemistry, 36(3), Article e6548. DOI: 10.1002/aoc.6548
9. Qurrat-ul-ain, R., Ur Rahman, M., Javed, H. M., Hassan, S., Munir, T., & Asghar, R. (2024). Exploring sulfonamide derivatives, Schiff bases, and metal complexes as antimicrobial agents: A comprehensive review. Inorganic Chemistry Communications, 170, Article 113396. DOI: 10.1016/j.inoche.2024.113396
10. Adewale, T. S., & Abosede, O. O. (2026). Synthesis and characterization of some metal complexes of tetracycline, theophylline and cimetidine. Discover Chemistry, 3(1), Article 320. DOI: 10.1007/s44371-026-00732-3
11. AlBaheley, N. A., Ali, A. A., & Fahad, T. A. (2021). Synthesis, characterization, and spectroscopic properties of new azo dyes derived from Sulfamerazine based on β- diketones and azo-metal (II) complexes. Journal of Physics: Conference Series, 1999(1), Article 012017. DOI: 10.1088/1742-6596/1999/1/012017
12. Rozbicki, P., & Branowska, D. (2025). A Review on Sulfonamide Complexes with Metals: Their Pharmacological Potential as Anticancer Drugs. Pharmaceuticals, 18(9), Article 1414. DOI: 10.3390/ph18091414
13. Dhumad, A. M., Hassan, Q. M. A., Emshary, C. A., Fahad, T., Raheem, N. A., & Sultan, H. A. (2021). Nonlinear optical properties investigation of a newly synthesised Azo-(β)- diketone dye. Journal of Photochemistry and Photobiology A: Chemistry, 418, Article 113429. DOI: 10.1016/j.jphotochem.2021.113429
14. Al-Gburi, L. J., Al-Noor, T. H., & Abdalrazaq, E. A. (2025). Biological Activity of Metal Complexes of Sulfamethoxazole and Its Derivatives: A Literature Review. Ibn AL-Haitham Journal For Pure and Applied Sciences, 38(1), 326–341. DOI: 10.30526/37.1.3091
15. Elbadawy, H. A., Eldissouky, A., El-Apasery, M. A., Elsayed, D. S., & Alaswad, E. A. (2025). Synthesis, characterization, computational and dyeing behavior of Cu (II) and Zn(II) metal complexes derived from azo-Schiff bases containing phenol derivatives. BMC Chemistry, 19(1), Article 207. DOI: 10.1186/s13065-025-01571-6
16. McCormack, A. T., & Stephens, J. C. (2024). The continuous flow synthesis of azos. Journal of Flow Chemistry, 14(2), 377–396. DOI: 10.1007/s41981-024-00307-2
17. Sherif, S., Aboelnaga, A., Elshemy, N. S., Elabbady, S., & Ramadan, S. K. (2026). Design and synthesis of novel sulfa-azo dyes: a sustainable approach to textile dyeing combined with microwave energy. RSC Advances, 16(6), 5374–5400. DOI: 10.1039/d5ra09499b
18. Obaid, S. M. H., Abd-Almonuim, A. E., Al-Naymi, H. A. S., Jarad, A. J., & Saleh, M. M. (2024). Synthesis and characterisation of metal ion complexes with a mixed ligand of azo dye and metformin; evaluation of their effectiveness against the growth of some clinically isolated pathogenic bacteria; and study of their toxicity on normal and cancerous Hepatocytes. Heliyon, 10(18), Article e37849. DOI: 10.1016/j.heliyon.2024.e37849
19. Gulcin, İ. (2020). Antioxidants and antioxidant methods: an updated overview. Archives of Toxicology, 94(3), 651–715. DOI: 10.1007/s00204-020-02689-3
20. Clinical and Laboratory Standards Institute. (2018). Performance standards for antimicrobial susceptibility testing (28th ed., CLSI supplement M100). Clinical and Laboratory Standards Institute. https://www.scirp.org/reference/referencespapers?referenceid=3501341
21. Kasare, M. S., Dhavan, P. P., Jadhav, B. L., & Pawar, S. D. (2019). Synthesis of Azo Schiff Base Ligands and Their Ni(II), Cu(II) and Zn(II) Metal Complexes as Highly-Active Antibacterial Agents. ChemistrySelect, 4(36), 10792–10797. DOI: 10.1002/slct.201901605
22. Iroka, C. G., Chioma, F., Amadi, J. U., Uzoekwe, N. M., & Egbujor, M. C. (2026). Synthesis, characterization, antimicrobial, and corrosion inhibition studies of divalent complexes of 2-((5-chloro-2-hydroxyphenyl) amino) naphthalene-1,4-dione chelator. Discover Chemistry, 3(1), Article 447. DOI: 10.1007/s44371-026-00836-w
23. Masoud, M. S., Hemdan, S. S., & Elsamra, R. M. I. (2023). Synthesis, Ligating Properties, Thermal Behaviour, Computational and Biological Studies of Some Azo-transition Metal Complexes. Journal of Inorganic and Organometallic Polymers and Materials, 33(1), 120–137. DOI: 10.1007/s10904-022-02483-x
24. Esarev, I. V., Karge, B., Zeng, H., Lippmann, P., Jones, P. G., Schrey, H., Brönstrup, M., & Ott, I. (2024). Silver Organometallics that are Highly Potent Thioredoxin and Glutathione Reductase Inhibitors: Exploring the Correlations of Solution Chemistry with the Strong Antibacterial Effects. ACS Infectious Diseases, 10(5), 1753–1766. DOI: 10.1021/acsinfecdis.4c00104
25. Tian, A.-X., Ji, X.-B., Sun, N., Xiao, R., Zhao, Y.-Y., Ni, H.-P., Tian, Y., & Ying, J. (2017). Four New Coordination Polymers Constructed by 2-(4-Thiazolyl) benzimidazole and 1,3,5-Benzenetricarboxylic Acid. Journal of Chemical Crystallography, 47(1–2), 1–9. DOI: 10.1007/s10870-016-0674-7
26. Moreira, Jeniffer Meyer; Vieira, Sara dos Santos Félix; Correia, Gabriel de Deus; de Almeida, Leandro Nascimento; Finoto, Simone; Brandl, Cândida Alíssia; Msumange, Aujenus Albert; Galvão, Fernanda; Pires de Oliveira, Kelly Mari; Paveglio, Guilherme Caneppele; da Silva, Monize Martins; Tirloni, Bárbara; de Carvalho, Cláudio Teodoro; & Roman, Daiane. (2025). Synthesis and Characterization of Novel Hydrazone Complexes: Exploring DNA/BSA Binding and Antimicrobial Potential. ACS Omega, 10(7), 7428–7440. DOI: 10.1021/acsomega.5c00069
27. Mujahid, M., Trendafilova, N., Rosair, G., Kavanagh, K., Walsh, M., Creaven, B. S., & Georgieva, I. (2023). Structural and Spectroscopic Study of New Copper (II) and Zinc(II) Complexes of Coumarin Oxyacetate Ligands and Determination of Their Antimicrobial Activity. Molecules, 28(11), Article 4560. DOI: 10.3390/molecules28114560
28. Islam, M. A., Tasnim, F., Biswas, M. T., Hossain, M. S., Hosen, M. E., Islam, M. R., Asraf, M. A., Hossen, M. F., Al-Dies, A.-A. M., Kudrat-E-Zahan, M., Tóth, Z., & Zaki, M. E. A. (2026). Structural elucidation, biological significance and computational approach of copper(ii), Nickel(ii) and Cobalt(ii) with bidentate Schiff base of N-(Naphthalene-1-ylmethylene) isonicotinohydrazide. Scientific Reports, 16(1), Article 3893. DOI: 10.1038/s41598-025-23208-3
29. Hchicha, K., Msalmi, R., Korb, M., Wahbi, H., Čižmár, E., Hamdi, M., & Naïli, H. (2024). Comprehensive Exploration of Optics and Magnetism in a Hydrothermally Synthesized Nickel (II) Complex. ACS Omega, 9(27), 29310–29319. DOI: 10.1021/acsomega.4c00421
30. Mitu, T. F., Islam, S., Akther, S., Jamal, A. H. M. S. I. M., Moulick, S. P., Uddin, M. N., Shaikh, M. A. A., & Bakshi, P. K. (2025). Synthesis and Characterization of Mn (II), Ni (II), and Cu (II) Complexes Derived from Sulfonamide and o-Vanillin-Based Schiff Base and Their Antimicrobial, Antioxidant, and Cytotoxic Properties. Applied Organometallic Chemistry, 39(6), Article e70203. DOI: 10.1002/aoc.70203
31. Aziz, K. N., Ahmed, K. M., Omer, R. A., Qader, A. F., & Abdulkareem, E. I. (2025). A review of coordination compounds: structure,

© Copyright: All rights reserved.

stability, and biological significance. Reviews in Inorganic Chemistry, 45(1), 1–19. DOI: 10.1515/revic-2024-0035
32. El-Gammal, O. A., El-Bindary, A. A., Eldesoky, A. M., & Abd Al-Gader, I. M. (2025). Synthesis, characterization, molecular docking and in vitro antibacterial assessments of anthracene-bis(hydrazine)thiosemicarbazide complexes with Co(II), Ni(II) and Cu(II) ions. Journal of Molecular Structure, 1322, Article 140339. DOI: 10.1016/j.molstruc.2024.140339
33. Fetouh, H. A., El-Mossalamy, E. H., El Desouky, J. M., & Batouti, M. E. (2024). Synthesis and characterization of new organometallic lanthanides metal complexes for photodynamic therapy. Scientific Reports, 14(1), Article 26184. DOI: 10.1038/s41598-024-75800-8
34. Mishra, D. P., Sahu, P. K., Sarangi, A. K., & Deb, D. K. (2025). Novel sulfonamide-based azo-metal complexes: Synthesis, characterization, theoretical studies, and In Vitro antioxidant and anticancer evaluation. Next Materials, 8, Article 100728. DOI: 10.1016/j.nxmate.2025.100728
35. Mohammed, L. A., Mahdi, N. I., & Aldujaili, R. A. B. (2020). Preparation, Characterization and the Biological Activity Study of a New Heterocyclic (Azo-Schiff Base) Ligand and Their Complexation with {Co, Ni, Cu, Zn(II)} Ions. Egyptian Journal of Chemistry, 63(1), 289–300. DOI: 10.21608/ejchem.2019.19821.2195
36. Lashanizadegan, M., Asna Ashari, H., Sarkheil, M., Anafcheh, M., & Jahangiry, S. (2021). New Cu(II), Co(II) and Ni(II) azo-Schiff base complexes: Synthesis, characterization, catalytic oxidation of alkenes and DFT study. Polyhedron, 200, Article 115148. DOI: 10.1016/j.poly.2021.115148
37. Maldonado, T., Flores, E., Llanos, L., Aravena, D., Vega, A., Godoy, F., Aspée, A., Arancibia-Miranda, N., Ferraudi, G., & Gómez, A. (2022). Azo–hydrazone tautomerism in organometallic complexes triggered by a -Re(CO)3(L) core: A spectroscopic and theoretical study. Dyes and Pigments, 197, Article 109953. DOI: 10.1016/j.dyepig.2021.109953
38. Damade, K. (2022). Spectral Analysis of Azo Derivatives for their Colourimetric Response to some Special Metal Ions. Letters in Applied NanoBioScience, 11(3), 3909–3916. DOI: 10.33263/LIANBS113.39093916
39. Iguchi, D., Ravelli, D., Erra-Balsells, R., & Bonesi, S. M. (2020). Substituent Effects on NMR Spectroscopy of 2,2-Dimethylchroman-4-one Derivatives: Experimental and Theoretical Studies. Molecules, 25(9), Article 2061. DOI: 10.3390/molecules25092061
40. Da Silva, H. C., Hernandes, I. S., & De Almeida, W. B. (2025). Quantum Chemical NMR Spectroscopic Structural Analysis in Solution: The Investigation of 3-Indoleacetic Acid Dimer Formation in Chloroform and DMSO Solution. Magnetic Resonance in Chemistry, 63(4), 292–313. DOI: 10.1002/mrc.5511
41. Venkatesh, G., Vennila, P., Kaya, S., Ben Ahmed, S., Sumathi, P., Siva, V., Rajendran, P., & Kamal, C. (2024). Synthesis and Spectroscopic Characterization of Schiff Base Metal Complexes, Biological Activity, and Molecular Docking Studies. ACS Omega, 9(7), 8123–8138. DOI: 10.1021/acsomega.3c08526
42. Gross, J. H. (2017). Mass Spectrometry: A Textbook (3rd ed.). Springer International Publishing. DOI: 10.1007/978-3-319-54398-7
43. Kokotou, M. G. (2020). Study of the Fragmentation Pathways of Sulfonamides by High-resolution Mass Spectrometry: Application to their Detection in Plasma by Direct Infusion. Current Pharmaceutical Analysis, 16(5), 513–519. DOI: 10.2174/1573412915666181205115350
44. Millbern, Z., Trettin, A., Wu, R., Demmler, M., & Vinueza, N. R. (2024). Synthetic dyes: A mass spectrometry approach and applications. Mass Spectrometry Reviews, 43(2), 327–344. DOI: 10.1002/mas.21818
45. Le, M. T., Morato, N. M., Kaerner, A., Welch, C. J., & Cooks, R. G. (2021). Fragmentation of Polyfunctional Compounds Recorded Using Automated High-Throughput Desorption Electrospray Ionization. Journal of the American Society for Mass Spectrometry, 32(8), 2261–2273. DOI: 10.1021/jasms.1c00176
46. Davidson, J. T., Piacentino, E. L., Sasiene, Z. J., Abiedalla, Y., DeRuiter, J., Clark, C. R., Berden, G., Oomens, J., Ryzhov, V., & Jackson, G. P. (2020). Identification of novel fragmentation pathways and fragment ion structures in the tandem mass spectra of protonated synthetic cathinones. Forensic Chemistry, 19, Article 100245. DOI: 10.1016/j.forc.2020.100245
47. Chai, Y., Shao, Y., Wang, L., & Wang, L. (2017). Loss of benzaldehyde in the fragmentation of protonated benzoylamines: Benzoyl cation as a hydride acceptor in the gas phase. Journal of Mass Spectrometry, 52(10), 664–671. DOI: 10.1002/jms.3969
48. Walencik, P. K., Choińska, R., Gołębiewska, E., & Kalinowska, M. (2024). Metal–Flavonoid Interactions—From Simple Complexes to Advanced Systems. Molecules, 29(11), Article 2573. DOI: 10.3390/molecules29112573
49. Damena, T., Alem, M. B., Zeleke, D., Desalegn, T., Eswaramoorthy, R., & Demissie, T. B. (2022). Novel Zinc(II) and Copper(II) Complexes of 2-((2-Hydroxyethyl) amino)quinoline-3-carbaldehyde for Antibacterial and Antioxidant Activities: A Combined Experimental, DFT, and Docking Study. ACS Omega, 7(30), 26336–26352. DOI: 10.1021/acsomega.2c02205
50. Abd El-Lateef, H. M., El-Dabea, T., Khalaf, M. M., & Abu-Dief, A. M. (2023). Recent Overview of Potent Antioxidant Activity of Coordination Compounds. Antioxidants, 12(2), Article 213. DOI: 10.3390/antiox12020213
51. Hasi, Q.-M., Fan, Y., Yao, X.-Q., Hu, D.-C., & Liu, J.-C. (2016). Synthesis, characterization, antioxidant and antimicrobial activities of a bidentate Schiff base ligand and its metal complexes. Polyhedron, 109, 75–80. DOI: 10.1016/j.poly.2016.01.052
52. Alhussaini, M. S., Alyahya, A. A. I., & Al-Ghanayem, A. A. (2025). Chelation-driven antimicrobial potency of Cu(II) complexes with N- and O- donor ligands: A review (2022–2025). Dyes and Pigments, 243, Article 113040. DOI: 10.1016/j.dyepig.2025.113040
53. Ashraf, J., & Riaz, M. A. (2022). Biological potential of copper complexes: a review. Turkish Journal of Chemistry, 46(3), 595–623. DOI: 10.55730/1300-0527.3356
54. F. Hadjer, B. Tahar, A. Djallal Eddine, & D. Sofiane. (2018). Antioxidant and Antimicrobial Activity of Some Transition Metal Complexes with Non-natural Amino Acids Used as Ligands. Journal of Materials and Environmental Science, 9(7), 2153–2157. https://www.jmaterenvironsci.com/Document/vol9/vol9_N7/235-JMES-3717-Hadjer.pdf
55. Orta-Rivera, A. M., Meléndez-Contés, Y., Medina-Berríos, N., Gómez-Cardona, A. M., Ramos-Rodríguez, A., Cruz-Santiago, C., González-Dumeng, C., López, J., Escribano, J., Rivera-Otero, J. J., Díaz-Rivera, J., Díaz-Vélez, S. C., Feliciano-Delgado, Z., & Tinoco, A. D. (2023). Copper-Based Antibiotic Strategies: Exploring Applications in the Hospital Setting and the Targeting of Cu Regulatory Pathways and Current Drug Design Trends. Inorganics, 11(6), Article 252. DOI: 10.3390/inorganics11060252
56. Kasim, S. M., Al-Dabbagh, B. M., Al-Shakarchi, W., & Mustafa, Y. F. (2023). Synthesis, characterization and biological evaluation of new azo-coumarinic derivatives. Applied Nanoscience, 13(2), 1095–1102. DOI: 10.1007/s13204-021-01873-w
57. El-Ghamry, H. A., Al-Ziyadi, R. O., Alkhatib, F. M., Takroni, K. M., & Khedr, A. M. (2023). Metal Chelates of Sulfafurazole Azo Dye Derivative: Synthesis, Structure Affirmation, Antimicrobial, Antitumor, DNA Binding, and Molecular Docking Simulation. Bioinorganic Chemistry and Applications, 2023, Article 2239976. DOI: 10.1155/2023/2239976

AUTHOR'S PROFILE



Dr. Noor Abdul-Hakim Abdul-Razzaq is an Iraqi academic and researcher specializing in chemical sciences. She earned a PhD in Chemistry from the College of Education for Pure Sciences at the University of Basrah. Her scientific contributions focus on analytical chemistry specifically, synthesising and characterising azo dye complexes and their biological and medical applications—as well as determining nutrients using ion chromatography techniques. Dr. Noor has served for several years as a high school principal under the General Directorate of Education in Basrah (Ministry of Education). She has participated in numerous scientific seminars and workshops at the University of Basrah. She has also served as an academic instructor for various training courses organized by the Basrah Directorate of Education.

Disclaimer/Publisher's Note: The statements, opinions, and data contained in all publications are solely those of the individual author(s) and contributor(s) and not of the Publisher /Journal and/or the editor(s). The Publisher /Journal and/or the editor(s) disclaim responsibility for any injury to people or property resulting from any ideas, methods, instructions, or products referred to in the content.

© Copyright: All rights reserved.